A multicomponent model for the optical to γ-ray emission from the Crab Pulsar

Riccardo Campana[1], **Enrico Massaro**[1], **Giancarlo Cusumano**[2], **and Teresa Mineo**[2]

[1] *Department of Physics, University of Rome "La Sapienza", Rome, Italy*
[2] *INAF – IASF-Pa, Palermo, Italy*

Abstract

We present a multicomponent model to explain the features of the pulsed emission and spectrum of the Crab Pulsar, on the basis of X and γ-ray observations performed with BeppoSAX, INTEGRAL and CGRO. This model explains the evolution of the pulse shape and of the phase-resolved spectra, ranging from the optical/UV to the GeV energy band, on the assumption that the observed emission is due to more components. The first component, C_O, is assumed to have the pulsed double-peaked profile observed at the optical frequencies, while the second component, C_X, is dominant in the interpeak and second peak phase regions. The spectra of these components are modelled with log-parabolic laws. Moreover, to explain the properties of the pulsed emission in the MeV-GeV band, we introduce two more components, $C_{O\gamma}$ and $C_{X\gamma}$, with phase distributions similar to those of C_O and C_X and log-parabolic spectra with the same curvature but different peak energies. This multicomponent model is able to reproduce both the broadband phase-resolved spectral behaviour and the changes of the pulse shape with energy. We also propose some possible physical interpretations in which C_O and C_X are emitted by secondary pairs via synchrotron mechanism while $C_{O\gamma}$ and $C_{X\gamma}$ can originate either from Compton scattered or primary curvature photons.

Introduction

The Crab Pulsar (PSR B0531+21) is perhaps the best known rotation-powered pulsar. It has a 33 ms period, and pulsed emission is detected throughout the whole electromagnetic spectrum, from the radio band to high energy gamma rays. The pulse has a characteristic double peak structure with a phase separation of 0.4.

It is well known that the pulse shape of the Crab changes with energy in the X and soft gamma-ray ranges where the emission of the second peak (P2) becomes higher than the first one (P1), and where it is present a significant emission from the region between the two peaks (bridge or interpeak, IP). This behaviour continues up to about 10 MeV, where the pulse almost sharply returns to a shape similar to the optical light curve. A satisfactory explanation for these changes has not been found so far.

On the basis of high quality BeppoSAX data, covering the wide energy range from 0.1 to 300 keV, we already proposed a two component model (Massaro *et al.*, 2000) to explain this behaviour. Here we extend this model, building upon a reanalysis of the whole set of BeppoSAX Crab observations. We found that the energy spectra of these components are not described by a simple power law, but show a spectral steepening towards high energies. We model these components with log-parabolic spectral distributions. The observations of BeppoSAX are thus well fitted. Moreover, to explain the behaviour in the MeV/GeV band, two more components are introduced, both with a similar shape and spectrum of the X-ray counterparts.

The two-component model: optical to hard X-rays

The first component, called C_O, is assumed to have the same pulsed profile observed at optical frequencies, while the second component, C_X, is described by an analytical model whose shape is determined by comparing $C_O + C_X$ with the observed pulse profiles, and that dominates at the interpeak (IP) and second peak (P2) phase regions (fig. 1). X-ray light curves are thus well reproduced (Massaro *et al.*. 2000).

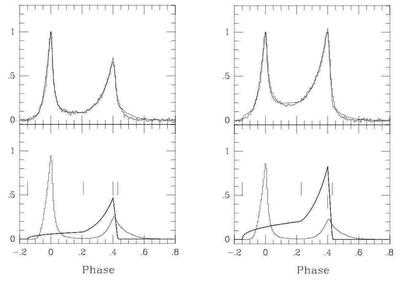

Figure 1: The two components C_O and C_X of the model at the energies of 8.85 keV (left) and 75.2 keV (right). In the upper panels: the model compared with BeppoSAX data. In the lower panels: C_O and C_X (from Massaro *et al.*, 2000).

Using the high-statistics observations of BeppoSAX we performed a phase-resolved spectral analysis and found that the photon indices of P1, P2 and IP are changing with energy, and linearly increasing with LogE (fig. 2).

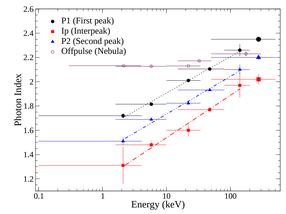

Figure 2: Photon indices of P1, IP and P2 as measured by the four NFI of BeppoSAX and by INTEGRAL-ISGRI.

We found that the spectra of C_O and C_X are well fitted by a log-parabolic spectral law,

$$F(E) = KE^{-(a+b\mathrm{Log}E)} \qquad (1)$$

where K is the flux at 1 keV and E is the energy in keV. The parameter b describes the "curvature" of the log-parabola. The energy-dependent spectral index can be obtained from the previous equation: $\alpha(E) = a + 2b\mathrm{Log}E$. According to this spectral law, the spectral energy distribution (SED) has a maximum at the energy $E_p = 10^{(2-a)/2b}$.

Extension of the model to the MeV/GeV band: needs for two more components

CGRO COMPTEL and EGRET observations (Kuiper *et al.*, 2001; Thompson, 2003) provided above ∼10 MeV light curves of a good statistical quality which show that the pulse shape turns to be similar to that of C_O, although some minor differences are present. At energies higher than ∼500 MeV the emission from IP and P2 increases, and this seems to reproduce the behaviour of the X-ray emission. In order to explain such a finding, we assume that there are two more, high-energy spectral components, $C_{O\gamma}$ and $C_{X\gamma}$, both with a log-parabolic spectral distribution and with the same pulse shape of the lower-energy components C_O and C_X. To be consistent with the upper limits to TeV pulsed emission (e.g. Lessard *et al.*, 2000) we added also an exponential cutoff to both $C_{O\gamma}$ and $C_{X\gamma}$, at the energy $E_c = 15$ GeV. This model therefore has 6 adjustable parameters, i.e. the normalizations, peak energies and curvatures of the $C_{O\gamma}$ and $C_{X\gamma}$ components. Assuming that the curvatures are equal to the C_O and C_X ones ($b = 0.16$), we are then able to well reproduce the broadband energy spectrum of the total (averaged) pulse and of the P1, IP and P2 phase regions (see fig. 3) and the ratios of P2/P1 and IP/P1 fluxes (in the same phase intervals of Kuiper *et al.*, 2001; fig. 4). We stress that there is no constraint on E_c: in fig. 4 (left) we plot also the P2/P1 ratio for various values of $C_{O\gamma}$ cutoff energy ranging from 9 to 15 GeV.

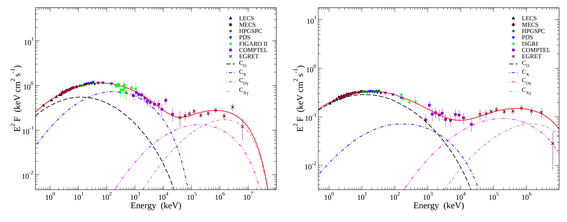

Figure 3: Broadband spectra of the total averaged pulse and of P1 with the four components of the model.

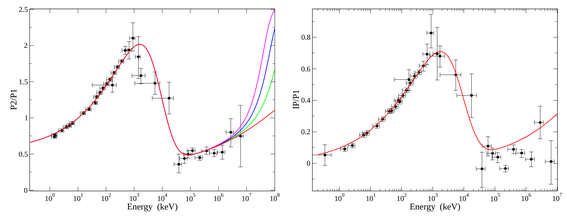

Figure 4: P2/P1 (left) and IP/P1 (right) ratios as derived from the model. Data points come from various experiments (Kuiper et al 2001).

Physical interpretation

The open question is the physical origin of these components that phenomenologically well explain the observations, in the framework of the high-energy pulsar emission models, either in the polar cap or outer gap models (e.g. Cheng *et al.*, 2000; Zhang & Cheng, 2002). Assuming that the lower-energy components C_O and C_X are produced by synchrotron emission of secondary electron-positron pairs created in the pulsar magnetosphere, the higher-energy components $C_{O\gamma}$ and $C_{X\gamma}$ could be due to:

- Emission of curvature radiation from primary particles accelerated in the electrostatic gap.
- Emission from inverse Compton scattering of the synchrotron photons by the secondary pairs themselves (Synchrotron-Self-Compton mechanism).

The different shape of the "O" and the "X" components is presumably due to the different location in the magnetosphere of the emission regions.

Conclusions

This model is able to give a consistent interpretation of the various peculiarities inherent to the high energy emission from the Crab Pulsar. Clearly, it is only a phenomenological model, but it could furnish some constraints to more detailed, physically-based emission models. In particular it is important to verify whether at energies higher than ∼1 GeV the pulse shape tends to be dominated by $C_{X\gamma}$. The GLAST/LAT experiment (Gehrels *et al.*, 1999), with its large collecting area, will give us very useful data in this range that will permit to better estimate the model parameters. Another interesting perspective is the adaptation of the model to other pulsars.

References

[1] Cheng K. S., Ruderman M., and Zhang L., *ApJ*, **537**, 964-976, (2000).

[2] Gehrels N., Michelson P., *et al.*., *Aph*, **11**, 277-282, (1999).

[3] Kuiper L., Hermsen W., Cusumano G., *et al.*., *A&A*, **378**, 918-935, (2001).

[4] Lessard R. W., Bond I. H., Bradbury S. M., *et al.*., *ApJ*, **531**, 942-948, (2000).

[5] Massaro E., Cusumano G., Litterio M., and Mineo T., *A&A*, **375**, 397-404, (2000).

[6] Thompson D. J., in *Cosmic Gamma Ray Sources*, Kluwer ASSL series, **304**, edited by K. Cheng and G. Romero, (2003)

[7] Zhang L. and Cheng K. S., *ApJ*, **569**, 872-877, (2002).